Heliyon 9 (2023) e21805

Contents lists available at ScienceDirect

Heliyon

journal homepage: www.cell.com/heliyon

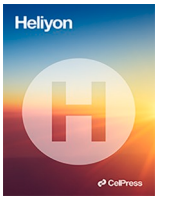

Powder properties of carbon-based solid acid catalyst for designing cellulose hydrolysis reactor with stirring apparatus

Daizo Yamaguchi

National Institute of Technology, Tsuyama College, 624-1, Numa, Tsuyama-City, Okayama 708-8509, Japan

A R T I C L E I N F O

Keywords:
Carbon-based solid acid catalyst
Flowability
Floodability
Adherence
Cellulose hydrolysis

A B S T R A C T

The powder properties of a carbon-based solid acid catalyst, an amorphous carbon material bearing SO_3H, COOH and OH groups, were investigated for the hydrolysis of cellulose. The Carr flowability and floodability indices, the angle of internal friction (adherence), and the particle size distribution and shape for the powder catalyst were determined. The need to develop a special reactor with a stirring apparatus for the hydrolysis of cellulose was determined based on the Carr flowability index. Insight into the interaction or adherence between the catalyst and crystalline cellulose during the hydrolysis process was gained by measuring the internal friction angle. The optimum moisture content in the catalyst to achieve the maximum adherence was investigated.

1. Introduction

Sugars obtained from the hydrolysis of lignocellulosic material are promising compounds for the production of important chemicals such as cellulosic ethanol, hydrocarbons, and starting materials for polymers associated with reducing CO_2 emissions and promoting sustainable green chemistry [1–5]. Substantial effort has been devoted to the development of appropriate hydrolysis schemes, including catalysis using mineral acids [6–8], enzyme-driven reactions [9,10], subcritical and supercritical water [11–14], carbon-based solid acid catalysts [3,15], magnetic mesoporous carbon-based solid acid catalysts [16], and cellulase-mimetic solid catalysts [17,18]. The hydrolysis of cellulose is usually catalyzed by sulfuric acid, the neutralization of which requires special processing that involves costly and inefficient catalyst separation from homogeneous reaction mixtures, and yields non-recyclable sulfate waste. In contrast, solid acid particles are readily separated from liquid products by decantation or filtration; such a solid catalyst can, without the need for neutralization, be repeatedly reused effectively, minimizing energy consumption and waste. The need for a "green" approach to chemical processing has stimulated the use of recyclable, strong solid acids instead of non-recyclable liquid acid catalysts such as H_2SO_4 [3,4,16,19–27].

We have demonstrated that an amorphous carbon material bearing SO_3H, COOH and OH groups functions as an efficient solid catalyst for the hydrolysis of cellulose at 343−373 K [15]. Just as mineral acid catalysts do, this carbon catalyst can hydrolyze not only pure crystalline cellulose, but also natural lignocellulosic reactants (such as eucalyptus or straw tips) into water-soluble β-1,4 glucan which is, in turn, hydrolyzed into glucose [15]. The high catalytic performance of the carbon-based solid acid catalyst is attributable to its capability to adsorb β-1,4 glucan and cellulose [15,28]. The surface of the catalyst readily adsorbs cellulose and water-soluble β-1,4 glucan, the hydrolytic product of cellulose, through hydrogen bonds between OH groups in the catalyst and cellulose or glucan. Strongly acidic SO_3H groups bonded to the catalyst function as effective active sites for decomposing strong hydrogen bonds and

E-mail address: tnt_yama@tsuyama-ct.ac.jp.

https://doi.org/10.1016/j.heliyon.2023.e21805
Received 7 August 2023; Received in revised form 11 October 2023; Accepted 29 October 2023
Available online 4 November 2023

hydrolyzing β-1,4 glycosidic bonds in cellulose or in β-1,4 glucan, resulting in efficient conversion of cellulose into glucose [15,28]. This is attributed to the incorporation of a large amount of water in the carbon bulk, which causes swelling of the catalyst. H_2O vapor adsorption isotherm (293 K) analyses have revealed that before sulfonation, partially carbonized cellulose has only a moderate ability to adsorb H_2O, whereas the sulfonated carbon material bearing SO_3H, COOH, and OH is able to adsorb a large amount of water [28]. The effective surface area of the carbon-based solid acid catalyst in the hydrolysis reaction (580 $m^2 g^{-1}$), which occurs in the presence of excess H_2O, is considerably higher than the BET surface area measured after dehydration (2 $m^2 g^{-1}$) [28]. This is attributable to the high density of hydrophilic functional groups bound to the flexible graphene clusters, and provides good access of reactants in solution to the SO_3H groups in the carbon bulk, resulting in strong catalytic performance despite the relatively low specific surface area [28].

The optimal reaction conditions for the hydrolysis of crystalline cellulose using this carbon-based solid acid catalyst have been investigated through an artificial neural network (ANN) and response surface methodology (RSM) [29]. The results revealed that the catalytic hydrolysis of cellulose proceeds in the same way as cellulose saccharification by concentrated H_2SO_4, with the reaction being highly dependent on the amount of water [29]. The glucose yield in the heterogeneous catalytic reaction reaches a maximum when the weight of water is comparable to that of the solid catalyst. A less than optimal amount of water is conducive to decomposing the β-1,4 glycosidic bonds and the strong hydrogen bonds in cellulose into water-soluble β-1,4 glucan. However, from the viewpoint of both kinetics and equilibrium, it is not conducive to the hydrolysis of water-soluble β-1,4 glucan into glucose [29].

A reactor equipped with a stirring apparatus for this catalytic reaction has been developed [29] and its basic properties have been investigated. The development of such a reactor for a solid-solid interface reaction with water (mostly adsorbed on the carbon-based solid acid catalyst) is a new challenge, although substantial effort has been devoted to the development of liquid-phase or solid-liquid-phase mixing reactors with a stirring apparatus [30–32]. In general, heterogeneous catalytic reactors place the emphasis on catalyst related factors, and heat and mass transfer. In the hydrolysis of cellulose with a carbon-based solid acid, reaction temperatures above 423 K should be avoided to prevent carbonization of the cellulose. In addition, a catalytic reaction with cellulose (a solid-solid interface reaction) must be achieved by stirring in a closed reactor while maintaining the optimum water content described above. The catalytic reaction is also inhibited by the presence of large amounts of water or gases, or apparatus corrosion. Under these constraints, slurry systems (stirred tanks, bubble columns), fixed-bed systems (trickle beds), jet loops, micron-channel reactors, and catalytic honeycomb monoliths, generally considered to be the most favorable, are not suitable reactors [33–35]. A specialized reactor is needed to overcome these constraints.

Here, we present the properties of a carbon-based solid acid catalyst in the form of a bulk powder, and investigate he grounds for developing a reactor with a stirring apparatus. Bulk powder materials have specific properties including particle size distribution, particle shape, bulk density, moisture content, surface area, cohesiveness, and hygroscopicity, each of which exhibits characteristic behavior during production and application. Knowledge of these properties is therefore essential for the manufacturer, the planning engineer, and the user with regard to the consistency of the quality of the product or acquisition of the data required for planning and designing the most efficient system for manufacturing bulk powder material. Especially important in this context are the characteristics of flow (flowability), flood (floodability) and viscosity (adherence).

Table 1
Point scores for evaluation of flowability [36].

Flowability and Performance	Angle of Repose		Compressibility		Angle of Spatula		Uniformity Coef.[a]		Cohesion[b]	
	Deg.	Points	%	Points	Deg.	Points	Units	Points	%	Points
Excellent, 90–100 pts.	25	25	5	25	25	25	1	25		
Aid not needed	26–29	24	6–9	23	26–30	24	2–4	23		
Will not arch	30	22.5	10	22.5	31	22.5	5	22.5		
Good, 80–90 pts.	31	22	11	22	32	22	6	22		
Aid not needed	32–34	21	12–14	21	33–37	21	7	21		
Will not arch	35	20	15	20	38	20	8	20		
Fair, 70–79 pts.	36	19.5	16	19.5	39	19.5	9	19		
Aid not needed (but	37–39	18	17–19	18	40–44	18	10–11	18		
vibrate if necessary)	40	17.5	20	17.5	45	17.5	12	17.5		
Passable, 60–69 pts.	41	17	21	17	46	17	13	17		
Borderline	42–44	16	22–24	16	47–59	16	15–16	16		
Material may hang up	45	15	25	15	60	15	17	15	<6	15
Poor, 40–59 pts.	46	14.5	26	14.5	61	14.5	18	14.5	6–9	14.5
Must agitate, vibrate	47–54	12	27–30	12	62–74	12	19–21	12	10–29	12
	55	10	31	10	75	10	22	10	30	10
Very poor, 20–39 pts.	56	9.5	32	9.5	76	9.5	23	9.5	31	9.5
Agitate	57–64	7	33–36	7	77–89	7	24–26	7	32–54	7
more positively	65	5	37	5	90	5	27	5	55	5
Very, very poor, 0-19 pts.	66	4.5	38	4.5	91	4.5	28	4.5	56	4.5
Special agit., hopper	67–89	2	39–45	2	92–99	2	29–35	2	57–79	2
or eng'g.	90	0	>45	0	>99	0	>36	0	>79	0

[a] Used with granular and powdered granular materials.
[b] Used with powders or where an effective cohesion can be measured.

2. Materials and methods

2.1. Carbon-based solid acid catalyst, crystalline cellulose and carbon

The carbon-based solid acid (an amorphous carbon material with SO_3H, COOH and OH groups) prepared by sulfonation of partially carbonized crystalline cellulose, and its structural information, were described previously [15,28,29]. Characterization confirmed that the resulting black powder (BET surface area, 2 $m^2\ g^{-1}$; true density, 1.66 g mL^{-1}) was amorphous carbon comprising SO_3H-, COOH- and phenolic OH-bearing nanographene sheets (*ca.* 1 nm) in a largely random distribution. The sample composition was $CH_{0.622}O_{0.540}S_{0.048}$, and the amounts of SO_3H, COOH and phenolic OH groups bonded to the graphene were 1.6, 0.8, and 5.0 mmol g^{-1}, respectively.

Since the moisture content of the catalyst has a marked effect on its catalytic activity [29], measurement of its physical properties was carried out for several moisture contents (dry (*ca.* 5 %), 20 %, 40 %, 60 %, 80 % 100 % by dry base). Appropriate amounts of water for the hydrolysis of cellulose were 1.5–3 mL for 3 g of the catalyst, with a 50–100 % moisture content being the suitable range [29]. Dried pure crystalline cellulose (Avicel®; crystallinity, 80 %; degree of polymerization, 200–300; true density, 1.53 g mL^{-1}) and dried partially carbonized crystalline cellulose (carbon (precursor of the catalyst); true density, 1.28 g mL^{-1}) were also used, and all measurements of physical properties were carried out under constant room temperature and humidity (293 K and 40 %).

2.2. Carr flowability and floodability indices

The Carr flowability index (Table 1) is derived from the angle of repose, compressibility, angle of spatula and uniformity (or cohesion). The floodability index (Table 2) is derived from the flowability index, angle of fall, angle of difference and dispersibility (Multi Tester MT-1001, Seishin Enterprise Co., Ltd.) [36]. Three supplementary values (aerated bulk density, packed bulk density, and uniformity) are also measured to obtain these indices [36]. These characteristic powder values are converted into 'point scores' and then the flowability and floodability indices are obtained as total point scores. The point score indicates the level of engineering intervention required when handling the powder.

2.3. Angle of internal friction by Jenike Johanson shearing test

Angles of internal friction (dynamic, φ; static, δ) and adherence (C) were determined by a direct shearing test (Jenike Johanson Flow Tester, Seishin Enterprise Co., Ltd.), and the values were calculated using the Mohr stress circle (Fig. 1) [37]. The friction coefficients for the carbon-based solid acid catalyst, carbon, and crystalline cellulose were assumed to be constant across all stress levels. The Coulomb equation was therefore established as the linear powder yield locus (*PYL*):

$$\tau = \sigma \tan \varphi + C \tag{1}$$

where τ is the shear stress, σ is the normal stress, φ is the angle of internal dynamic friction, and C is the adherence, with the powders assumed to be 'Coulomb powder'. The angle of internal static friction is defined as the angle of the critical state line (*CSL*), a straight

Table 2
Point scores for evaluation of floodability [36].

Floodability and Performance	Flowability		Angle of Fall		Angle of Difference		Dispersibility	
	Pts. (Table 1)	Points	Deg.	Points	Deg.	Points	%	Points
Very floodable, 80–100 pts.	60 +	25	10	25	30 +	25	50 +	25
Positive rotary seal	59–56	24	11–19	24	29–29	24	49–44	24
will be necessary	55	22.5	20	22.5	27	22.5	43	22.5
	54	22	21	22	26	22	42	22
	53–50	21	22–24	21	25	21	41–36	21
	49	20	25	20	24	20	35	20
Floodable, 60–79 pts.	48	19.5	26	19.5	23	19.5	34	19.5
Rotary seal will	47–45	18	27–29	18	22–20	18	33–29	18
be necessary	44	17.5	30	17.5	19	17.5	28	17.5
	43	17	31	17	18	17	27	17
	42–40	16	32–39	16	17–16	16	26–21	16
	39	15	40	15	15	15	20	15
Inclined to flood, 40–59 pts.	38	14.5	41	14.5	14	14.5	19	14.5
Rotary seal is desirable	37–34	12	42–49	12	13–11	12	18–11	12
	33	10	50	10	10	10	10	10
Could flood, 25–39 pts.	32	9.5	51	9.5	9	9.5	9	9.5
Rotary seal probably needed	31–29	8	52–56	8	8	8	8	8
depending on drop, veloc.	28	6.25	57	6.25	7	6.25	7	6.25
Non-floodable, 0–24 pts.	27	6	58	6	6	6	6	6
Rotary seal will	26–23	3	59–64	3	5–1	3	5–1	3
not be needed	<23	0	>64	0	0	0	0	0

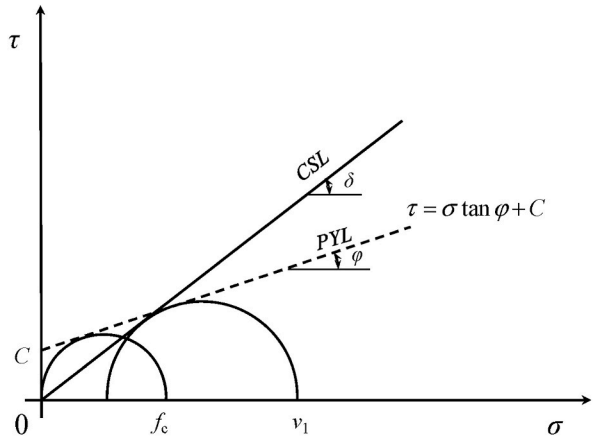

Fig. 1. Mohr stress circle (see Table 5) [37]. *PYL* denotes powder yield locus. *CSL* denotes critical state line. φ is the angle of internal dynamic friction, δ is the angle of significant internal friction, C is the adherence, f_c is the simple compression failure stress, and v_1 is the maximum principal stress.

line from the origin. A higher angle of internal friction indicates higher friction between powder layers. Coefficients of dynamic and static friction are defined as the values of tan φ and tan δ.

2.4. Particle size distribution and shape

The particle size distributions for the carbon-based solid acid catalyst and the crystallized cellulose were measured (Laser Micron Sizer (LMS-2000e), Seishin Enterprise Co., Ltd.) using water as the carrier fluid. The circle-equivalent diameter and the degree of circularity were also determined by image processing (PITA-1, Seishin Enterprise Co., Ltd.) using isopropyl alcohol was used as the carrier fluid. The magnification was set to 10× , and N8PL was used as the photochromatic filter. The circle-equivalent diameter was defined as the diameter of a circle of the same area as the projected area of the particle. The degree of circularity (d_c) was defined as follows:

$$d_c = 4\pi S / L^2 \tag{2}$$

where S is the projected area of the particle, and L is the boundary length of the projected area of the particle. The closer the degree of circularity is to 1, the closer the shape is to a circle.

3. Results and discussion

3.1. Carr flowability and floodability indices

The measured values of four different physical properties of each powder according to the Carr flowability index are shown in the odd columns in Table 3, and the points scored by each value of the flow property of the powder are shown in the even columns (see also Table 1). Based on the Carr index, flowability scores were allotted to seven categories as defined in Table 1. For example, the flowability of crystalline cellulose was evaluated at an angle of repose of 41.33°, scoring 17.0 points; compressibility at 36.47 %, scoring 7.0 points; angle of spatula at 75.67°, scoring 9.5 points; and uniformity coefficient at 3.83, scoring 23.0 points (since it exhibited no cohesion, the uniformity coefficient was used). Thus, with a total score of 56.5 points for flowability, this powder was evaluated as 'poor' (see Table 1) and requires remedial measures of agitation and vibration. The flowability of the water-bearing carbon-based solid acid catalyst (20–100 % moisture content) was 'very, very poor', in that its powder forms an arch in a hopper and, consequently, requires special agitation, hoppers or techniques for use in the hydrolysis of cellulose.

That the flowability of crystalline cellulose and carbon, i.e., the feedstock and precursor of the catalyst, is totally different from that of the catalyst, is attributable to the surface structure of the catalyst comprising SO_3H-, COOH- and phenolic OH-bearing nanographene sheets in a largely random distribution [15]. The catalyst can incorporate large amounts of water into the carbon bulk because of the high density of hydrophilic functional groups bound to the flexible nanographene sheets [15]. The amount of adsorbed H_2O at 1.5 kPa, which is much lower than the saturated water vapor pressure (*ca.* 3 kPa), exceeds 0.01 mol g^{-1} [15]. Assuming that the adsorption cross section of H_2O is 0.125 nm^2, the effective surface area of the catalyst is estimated to exceed 560 m^2 g^{-1} at this water vapor pressure [15]. Therefore, the adherence of the catalyst containing water is considered high; consequently, the flowability is 'very, very poor'.

Table 4 shows measured values for four different physical properties for the Carr floodability index. The floodability of a powder refers to its tendency to exhibit liquid-like flow due to the natural fluidization of particles by air [36]. Based on the Carr index, floodability scores were divided into five categories as shown in Table 2. For example, the floodability of crystalline cellulose was as

Table 3
Flowability of crystalline cellulose, carbon, and carbon-based solid acid catalyst.

Powder		Angle of Repose		Compressibility		Angle of Spatula		Uniformity Coef.		Cohesion		Flowability [a]	
		Deg.	Points	%	Points	Deg.	Points	Units	Points	%	Points	Points	Performance
Crystalline cellulose	Dry	41.33	17.0	36.47	7.0	75.67	9.5	3.83	23.0	–	–	56.5	Poor
Carbon	Dry	39.67	17.5	36.30	7.0	72.33	12.0	–	–	35.62	7.0	43.5	Poor
Carbon-based solid acid	Dry	45.33	15.0	40.04	2.0	65.17	12.0	–	–	58.92	2.0	31.0	Very poor
	20 %	61.00	7.0	46.07	0.0	93.83	2.0	–	–	99.80	0.0	9.0	Very, very poor
	40 %	54.67	10.0	46.57	0.0	94.50	2.0	–	–	100.0	0.0	12.0	Very, very poor
	60 %	55.33	10.0	45.86	0.0	93.17	2.0	–	–	100.0	0.0	12.0	Very, very poor
	80 %	51.67	12.0	41.75	2.0	91.67	2.0	–	–	100.0	0.0	16.0	Very, very poor
	100 %	50.67	12.0	39.31	2.0	91.67	2.0	–	–	100.0	0.0	16.0	Very, very poor

[a] See the first column of Table 1.

Table 4
Floodability of crystalline cellulose, carbon, and carbon-based solid acid catalyst.

Powder		Flowability		Angle of Fall		Angle of Difference		Dispersibility		Floodability [a]	
		Pts. (Table 3)	Points	Deg.	Points	Deg.	Points	%	Points	Points	Performance
Crystalline cellulose	Dry	56.5	24.0	22.67	21.0	18.67	17.5	25.50	16.0	78.5	Floodable
Carbon	Dry	43.5	17.5	18.00	24.0	21.67	18.0	26.70	17.0	76.5	Floodable
Carbon-based solid acid	Dry	31.0	8.0	22.00	21.0	23.33	19.5	47.60	24.0	72.5	Floodable
	20 %	9.0	0.0	37.33	16.0	23.67	20.0	13.60	12.0	48.0	Inclined to flood
	40 %	12.0	0.0	48.67	12.0	6.00	6.0	3.40	3.0	21.0	Non-floodable
	60 %	12.0	0.0	49.00	12.0	6.33	6.0	3.80	3.0	21.0	Non-floodable
	80 %	16.0	0.0	49.67	10.0	2.00	3.0	16.00	3.0	16.0	Non-floodable
	100 %	16.0	0.0	49.33	12.0	1.33	3.0	3.00	3.0	18.0	Non-floodable

[a] See the first column of Table 2.

follows: the flowability of 56.5 points scores 24.0 points; the angle of fall of 22.67°, scores 21.0 points; the angle of difference of 18.67° scores 17.5 points; and the dispersibility of 25.50 % scores 16.0 points. Thus, the total score of 78.5 indicates good floodability ('floodable') (see Table 2) and the need for a rotary seal in the apparatus for this powder.

Accordingly, the carbon and the dried catalyst were also evaluated as 'floodable', whereas the catalyst containing water, especially with a 40–100 % moisture content (suitable moisture content for the hydrolysis of cellulose), was evaluated as 'non-floodable' and would require a rotary seal in the apparatus. The decrease in the floodability of the carbon-based solid acid catalyst with increasing moisture content was attributed to its water adsorption capability. The sulfonated carbon material bearing SO_3H, COOH, and OH is able to adsorb a large amount of water, resulting in interactions between particles, attributable to the high density of hydrophilic functional groups bound to the flexible graphene clusters [28]. This resulted in a very, very poor flowability index and an evaluation as non-floodable from the floodability index at 40–100 % moisture content.

3.2. Angle of internal friction

Table 5 shows the results of measurements of the angle of internal friction using the Mohr stress circle. The coefficient of dynamic friction (tan φ) decreased from 0.7 to 0.5 with increasing moisture content (25–35° angle of internal dynamic friction in Table 5) from 40 to 100 %, the appropriate moisture content for the hydrolysis of cellulose (Fig. 2). The coefficient of static friction (tan δ) decreased from 1.0 to 1.5 (45–55° angle of internal static friction in Table 5) from 40 to 100 % moisture content. At 20 % moisture content, the value of both friction coefficients was almost the same (1.0) (Fig. 2) indicating low adherence.

The adherence, C, for a moisture content of 20 % was 0.8 kPa, reached a maximum (3.4 kPa) at 40 %, and then decreased (2.8 kPa) at 100 % (Table 5). The adherence (30–35 g cm^{-2}) under conditions suitable for the hydrolysis of cellulose and crystalline cellulose (29.5 g cm^{-2}) at 2.9 kPa provided valuable guidance for the design of the special reactor. The optimum moisture content (50–100 %) for the hydrolysis of cellulose using the catalyst described elsewhere [29] corresponded to that providing the maximum adherence, demonstrating that the catalyst and crystalline cellulose were interacting at *ca.* 3 kPa of adherence during the hydrolysis. The high catalytic performance in the reaction is attributable to the capability of the catalyst to adsorb β-1,4 glucan as well as cellulose [15], as confirmed in this study.

Despite the insignificant difference in powder properties between the catalyst in the dry state and the precursor carbon, the catalyst remains very difficult to handle in the presence of water, due to its adherence. The results of the flowability and floodability analyses are also significant for the design of production equipment. The relatively large adherence of the precursor carbon is attributed to electrostatic charges between the particles. A special reactor with a stirring apparatus providing twice the efficiency of a conventional apparatus has been developed with thin, light and tough blades suitable for the hydrolysis of cellulose by the catalyst, which is a solid-solid interface reaction.

Table 5
Angle of internal friction for crystalline cellulose, carbon, and carbon-based solid acid catalyst.

Powder		Consolidation pressure /kPa	Simple compression failure stress, f_c/kPa [a]	Maximum principal stress, ν_1/kPa [a]	Angle of internal dynamic friction, φ/° [a]	Angle of internal static friction, δ/° [a]	Adherence, C/kPa [a]
Crystalline cellulose		22.3	13.7	60.0	44.2	49.3	2.9
Carbon		4.8	9.9	15.4	45.8	62.8	2.0
Carbon-based solid acid	20 %	10.4	3.9	28.4	44.6	47.5	0.8
	40 %	10.4	12.5	18.8	33.3	55.3	3.4
	60 %	10.4	12.2	19.3	34.1	54.3	3.2
	80 %	10.4	10.4	17.6	30.5	49.9	3.0
	100 %	10.4	9.0	15.9	25.7	45.1	2.8

[a] See Fig. 1.

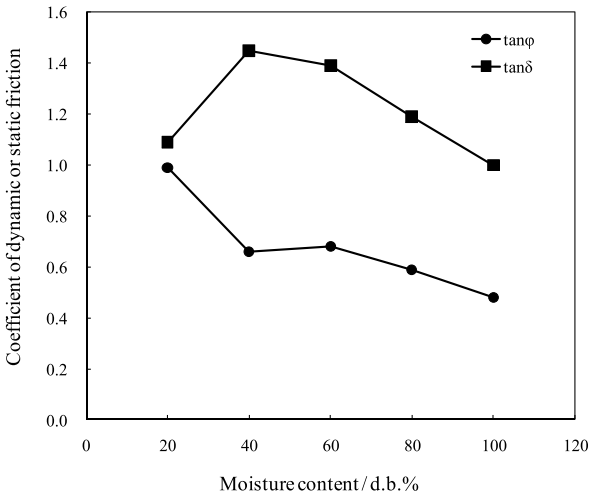

Fig. 2. Coefficients of dynamic (tan φ) and static (tan δ) friction for carbon-based solid acid catalyst.

3.3. Particle size distribution and shape

The particle size distribution for the catalyst was 2–200 μm and that of crystalline cellulose was 0.5–300 μm (Fig. 3). The average particle size (determined as the size at 50 % cumulative frequency (d(50)) for the catalyst was 47.97 μm and that for crystalline cellulose was 69.56 μm. The particle size of crystalline cellulose (as feedstock) decreased by *ca.* 30 % and its distribution was narrowed through carbonization and sulfonation.

Image processing yielded an average circle-equivalent diameter of 4.32 μm for the catalyst, while that for crystalline cellulose was 17.84 μm (Fig. 4). The average degree of circularity for the catalyst was 0.899, while that for crystalline cellulose was 0.687 (Fig. 5). Image processing showed that the strip shape for crystalline cellulose became circular following carbonization and sulfonation. These results are expected to be valuable in simulation studies for resolving the agitation problem for the hydrolysis of cellulose in a solid-solid interface reaction.

4. Conclusions

The powder properties of a carbon-based solid acid catalyst (an amorphous carbon material bearing SO_3H, COOH and OH groups) and those of crystalline cellulose (the substrate for the hydrolysis of cellulose and the feedstock for the catalyst) were investigated based on the Carr flowability and floodability indices, the angle of internal friction (adherence), and the particle distribution and shape for different moisture contents. The flowability of the catalyst containing water was 'very, very poor' necessitating a special reactor for the hydrolysis of cellulose. On the other hand, the floodability of the catalyst containing water was 'non-floodable', requiring no provisions. The catalyst and the crystalline cellulose interacted at *ca.* 3 kPa of adherence during the hydrolysis process, as demonstrated by the internal friction angle determined by the Mohr stress circle. The moisture content that gave a maximum adherence corresponded to the optimum value (50–100 %) for the hydrolysis of cellulose. Useful information was acquired for the development of a reactor with a stirring apparatus and for simulating agitation during the hydrolysis of cellulose. The evaluation methods in this study are also applicable to many novel functional materials, for example, heteroatom-doped carbon-based solid acids [38,39].

Data availability statement

Data will be made available on request.

CRediT authorship contribution statement

Daizo Yamaguchi: Conceptualization, Data curation, Formal analysis, Funding acquisition, Investigation, Methodology, Project administration, Resources, Software, Supervision, Validation, Visualization, Writing – original draft, Writing – review & editing.

Declaration of competing interest

The authors declare that they have no known competing financial interests or personal relationships that could have appeared to influence the work reported in this paper.

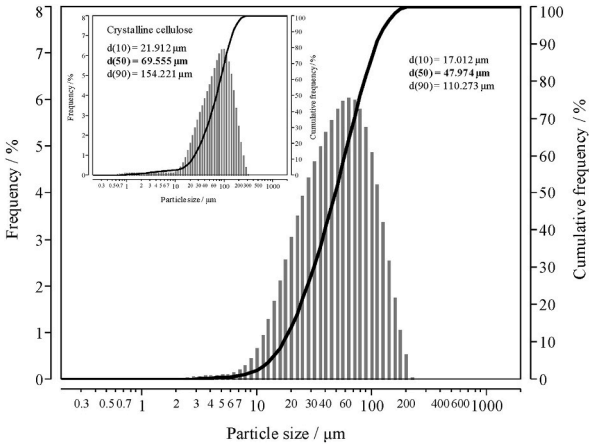

Fig. 3. Particle size distribution for carbon-based solid acid catalyst.

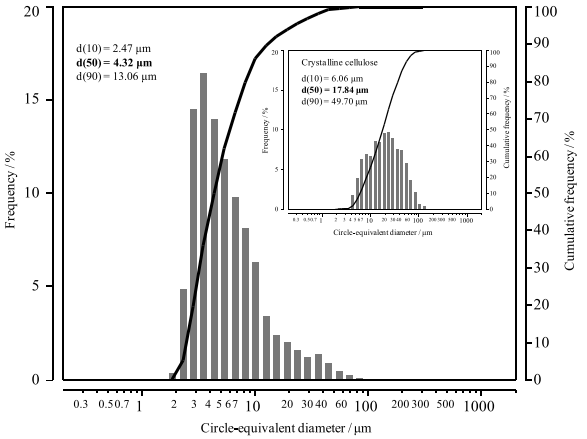

Fig. 4. Circle-equivalent diameter for carbon-based solid acid catalyst.

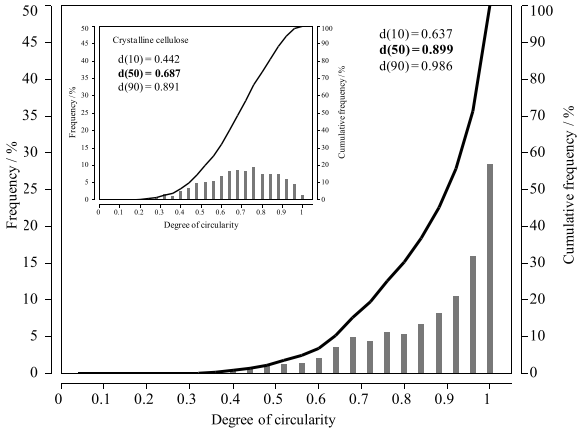

Fig. 5. Degree of circularity for carbon-based solid acid catalyst.

Acknowledgments

The author is grateful to Professor Michikazu Hara of the Tokyo Institute of Technology. This work was supported by the New Energy and Industrial Technology Development Organization (NEDO), Japan (grant no. 04A32502), the Research and Development in

a New Interdisciplinary Field Based on Nanotechnology and Materials Science programs of the Ministry of Education, Culture, Sports, Science and Technology (MEXT), Japan, and a Grant-in-Aid for Scientific Research (no. 18206081) from the Japan Society for the Promotion of Science (JSPS). The authors thank FORTE Science Communications (https://www.forte-science.co.jp/) for English language editing.

References

[1] B. Hahn-Hägerdal, M. Galbe, M.F. Gorwa-Grauslund, G. Lidén, G. Zacchi, Bio-ethanol – the fuel of tomorrow from the residues of today, Trends Biotechnol. 24 (12) (2006) 549–556, https://doi.org/10.1016/j.tibtech.2006.10.004.
[2] A.J. Ragauskas, C.K. Williams, B.H. Davison, G. Britovsek, J. Cairney, C.A. Eckert, W.J. Frederick, J.P. Hallett, D.J. Leak, C.L. Liotta, J.R. Mielenz, R. Murphy, R. Templer, T. Tschaplinski, The path forward for biofuels and biomaterials, Science 311 (5760) (2006) 484–489, https://doi.org/10.1126/science.11147.
[3] A. Mahajan, P. Gupta, Carbon-based solid acids: a review, Environ. Chem. Lett. 18 (2) (2020) 299–314, https://doi.org/10.1007/s10311-019-00940-7.
[4] W.G. Ramdani, A. Karam, K.O. Vigier, S. Rio, A. Ponchel, F. Jérôme, Catalytic glycosylation of glucose with alkyl alcohols over sulfonated mesoporous carbons, Mol. Catal. 468 (May) (2019) 125–129, https://doi.org/10.1016/j.mcat.2019.02.016.
[5] K. Nakajima, M. Hara, Environmentally benign production of chemicals and energy using a carbon-based strong solid acid, J. Am. Ceram. Soc. 90 (12) (2007) 3725–3734, https://doi.org/10.1111/j.1551-2916.2007.02082.x.
[6] W.L. Faith, Development of the scholler process in the United States, Ind. Eng. Chem. 37 (1) (1945) 9–11, https://doi.org/10.1021/ie50421a004.
[7] E.C. Sherrard, F.W. Kressman, Review of processes in the United States prior to world war II, Ind. Eng. Chem. 37 (1) (1945) 5–8, https://doi.org/10.1021/ie50421a003.
[8] E.E. Harris, E. Beglinger, Madison wood sugar process, Ind. Eng. Chem. 38 (9) (1946) 890–895, https://doi.org/10.1021/ie50441a012.
[9] Y.P. Zhang, L.R. Lynd, Toward an aggregated understanding of enzymatic hydrolysis of cellulose: noncomplexed cellulase systems, Biotechnol. Bioeng. 88 (7) (2004) 797–824, https://doi.org/10.1002/bit.20282.
[10] A.K. Patel, R.R. Singhania, S.J. Sim, A. Pandey, Thermostable cellulases: current status and perspectives, Bioresour. Technol. 279 (May) (2019) 385–392, https://doi.org/10.1016/j.biortech.2019.01.049.
[11] M. Sasaki, B. Kabyemela, R. Malaluan, S. Hirose, N. Takeda, T. Adschiri, K. Arai, Cellulose hydrolysis in subcritical and supercritical water, J. Supercrit. Fluids 13 (1–3) (1998) 261–268, https://doi.org/10.1016/S0896-8446(98)00060-6.
[12] M. Sasaki, Z. Fang, Y. Fukushima, T. Adschiri, K. Arai, Dissolution and hydrolysis of cellulose in subcritical and supercritical water, Ind. Eng. Chem. Res. 39 (8) (2000) 2883–2890, https://doi.org/10.1021/ie990690j.
[13] M. Sasaki, T. Adschiri, K. Arai, Kinetics of cellulose conversion at 25 MPa in sub- and supercritical water, Am. Inst. Chem. Eng. J. 50 (1) (2004) 192–202, https://doi.org/10.1002/aic.10018.
[14] Y. Liu, H. Fu, W. Zhang, H. Liu, Effect of crystalline structure on the catalytic hydrolysis of cellulose in subcritical water, ACS Sustain. Chem. Eng. 10 (18) (2022) 5859–5866, https://doi.org/10.1021/acssuschemeng.1c08703.
[15] S. Suganuma, K. Nakajima, M. Kitano, D. Yamaguchi, H. Kato, S. Hayashi, M. Hara, Hydrolysis of cellulose by amorphous carbon bearing SO_3H, COOH, and OH groups, J. Am. Chem. Soc. 130 (38) (2008) 12787–12793, https://doi.org/10.1021/ja803983h.
[16] D. Yamaguchi, K. Watanabe, S. Fukumi, Hydrolysis of cellulose by a mesoporous carbon-$Fe_2(SO_4)_3$/γ-Fe_2O_3 nanoparticle based solid acid catalyst, Sci. Rep. 6 (2016), 20327, https://doi.org/10.1038/srep20327.
[17] L. Shuai, X. Pan, Hydrolysis of cellulose by cellulase-mimetic solid catalyst, Energy Environ. Sci. 5 (May) (2012) 6889–6894, https://doi.org/10.1039/C2EE03373A.
[18] M. Tyufekchiev, P. Duan, K. Schmidt-Rohr, S.G. Focil, M.T. Timko, M.H. Emmert, Cellulase-Inspired solid acids for cellulose hydrolysis: structural explanations for high catalytic activity, ACS Catalsis 8 (2) (2018) 1464–1468, https://doi.org/10.1021/acscatal.7b04117.
[19] B. Harton, Green chemistry puts down roots, Nature 400 (6746) (1999) 797–799, https://doi.org/10.1038/23528.
[20] M. Misono, Acid catalysis for clean production. Green aspects of heteropolyacid catalysts, Comptes Rendus Acad. Sci. - Ser. IIC Chem. 3 (6) (2000) 471–475, https://doi.org/10.1016/S1387-1609(00)01165-8.
[21] P.T. Anastas, M.M. Kirchhoff, Origins, current status, and future challenges of green chemistry, Acc. Chem. Res. 35 (9) (2002) 686–694, https://doi.org/10.1021/ar010065m.
[22] J.H. Clark, Solid acid for green chemistry, Acc. Chem. Res. 35 (9) (2002) 791–797, https://doi.org/10.1021/ar010072a.
[23] J.M. DeSimone, Practical approaches to green solvents, Science 297 (5582) (2002) 799–803, https://doi.org/10.1126/science.1069622.
[24] T. Okuhara, Water-tolerant solid acid catalysts, Chem. Rev. 102 (10) (2002) 3641–3666, https://doi.org/10.1021/cr0103569.
[25] P.T. Anastas, J.B. Zimmermann, Sustainability requires objectives at the molecular, product, process, and system levels, Environ. Sci. Technol. 37 (5) (2003) 94A–101A, https://doi.org/10.1021/es032373g.
[26] K. Smith, G.A. El-Hiti, A.J. Jayne, M. Butters, Acetylation of aromatic ethers using acetic anhydride over solid acid catalysts in a solvent-free system. Scope of the reaction for substituted ethers, Organ. Biomol. Chem. 1 (9) (2003) 1560–1564, https://doi.org/10.1039/B301260C.
[27] M. Okamura, A. Takagaki, M. Toda, J.N. Kondo, K. Domen, T. Tatsumi, M. Hara, S. Hayashi, Acid-catalyzed reaction on flexible polycyclic aromatic carbon in amorphous carbon, Chem. Mater. 18 (13) (2006) 3039–3045, https://doi.org/10.1021/cm0605623.
[28] M. Kitano, D. Yamaguchi, S. Suganuma, K. Nakajima, H. Kato, S. Hayashi, M. Hara, Adsorption-enhanced hydrolysis of β-1,4-glucan on graphene-based amorphous carbon bearing SO_3H, COOH, and OH groups, Langmuir 25 (9) (2009) 5068–5075, https://doi.org/10.1021/la8040506.
[29] D. Yamaguchi, M. Kitano, S. Suganuma, K. Nakajima, H. Kato, M. Hara, Hydrolysis of cellulose by a solid acid catalyst under optimal reaction conditions, J. Phys. Chem. C 113 (8) (2009) 3181–3188, https://doi.org/10.1021/jp808676d.
[30] N. Harnby, M.F. Edwards, A.W. Nienow, Mixing in the Process Industries, Butterworth-Heinemann, Oxford, 1997, https://doi.org/10.1016/B978-0-7506-3760-2.X5020-3.
[31] E.L. Paul, V.A. Atiemo-Obeng, S.M. Kresta, Handbook of Industrial Mixing: Science and Practice, Wiley-Interscience, Hoboken, 2003, https://doi.org/10.1002/0471451452.
[32] Technical Information Institute Co., LTD, Latest Mixing Technology (Practice, Technical Information Institute Co., LTD, Tokyo, 2007 (in Japanese).
[33] E.H. Stitt, Alternative multiphase reactors for fine chemicals: a world beyond stirred tanks? Chem. Eng. J. 90 (No.1–2) (2002) 47–60, https://doi.org/10.1016/S1385-8947(02)00067-0.
[34] J. Poissonnier, A. Callewaert, K. Moonen, G.B. Marin, J.W. Thybaut, Comparison of jet loop and trickle-bed reactor performance in large-scale exploitation of glucose reductive aminolysis, Catal. Today 387 (2022) 119–127, https://doi.org/10.1016/j.cattod.2020.12.006. March.
[35] M. Schrimpf, J. Esteban, T. Rösler, A.J. Vorholt, W. Leitner, Intensified reactors for gas-liquid-liquid multiphase catalysis: from chemistry to engineering, Chem. Eng. J. 372 (2019) 917–939, https://doi.org/10.1016/j.cej.2019.03.133. September.
[36] R.L. Carr, Evaluating flow properties of solids, Chem. Eng. 72 (2) (1965) 163–168.
[37] J. Tsubaki, M. Suzuki, Y. Kanda, Particle and Powder Engineering, The Nikkan kogyo shinbun, LTD, Tokyo, 2002, pp. 159–181, in Japanese).
[38] J. Alom, Hasan, Md. Asaduzaman, M.T. Alam, D. Belhaj, R. Selvaraj, Md. A. Hossain, M. Zargar, M.B. Ahmed, Catalytical performance of heteroatom doped and undoped carbon-based materials, Catalysts,Vol.13, No.5. https://doi.org/10.3390/catal13050823.
[39] J. Duan, S. Chen, M. Jaroniec, S.Z. Qiao, Heteroatom-doped graphene-based materials for energy-relevant electrocatalytic processes, ACS Catalysis 5 (9) (2015) 5207–5234. https://doi.org/10.1021/acscatal.5b00991.